Ten different fields were randomly selected, and the number of stained vascular endothelial cells in each field was counted using a light microscope under high-power magnification (×200). The stained blood vessels from the 10 fields were averaged and the results expressed as vascular density (per square millimeter). The frozen sections were immunolabeled with primary antibodies, such as anti-cTNT (Abcam) and anti-slow myosin heavy chain (sMHC, Sigma-Aldrich Corp.), visualized with AlexaFluor488 goat anti-mouse IgG (Invitrogen) counterstained with DAPI, and assessed using the Biorevo BZ-9000 (Keyence) or confocal microscopy (Olympus Japan, FV1000-D IX81, Tokyo, Japan).

Fluorescence *in-situ* hybridization (FISH)

The paraffin-embedded sections were deparaffinized and incubated in 2× SSC for 5 minutes at room temperature (RT), then heated in a microwave oven for 10 minutes and cooled to RT. The samples were subsequently incubated in 0.1% pepsin/0.1M HCl for 5 minutes at 37°C, washed with PBS, and dehydrated through a series of ethanol solutions. A human-specific genomic FISH probe labeled with Cy3 (Chromosome Science Labo, Sapporo, Japan) was then applied to the samples. The entire cover slide with the probe was denatured at 95°C for 10 minutes and then hybridized at 37°C overnight. The following day, the samples were washed with 50% formamide/2× SSC at 37°C for 20 minutes and then with 1×SSC at RT for 15 minutes. The

sections were double-stained with the other antibodies described above and counterstained with DAPI.

Real-time PCR

Total RNA was extracted from cardiac tissue and reverse transcribed using TaqMan reverse transcription reagents (Applied Biosystems, Stockholm, Sweden), and real-time polymerase chain reaction (RT-PCR) was performed with the ABI PRISM 7700 (Applied Biosystems)[7] system using pig-specific primers for vascular endothelial growth factor (VEGF) and basic fibroblast growth factor (bFGF). cDNA samples were prepared and assayed in triplicate. The average copy number of gene transcripts was normalized to that of glyceraldehyde-3-phosphate dehydrogenase (GAPDH) for each sample.

Statistical analysis

JMP software (JMP7.01, SAS institute Inc., Cary, NC) was used for all statistical analyses. Continuous values are expressed as the mean ± standard deviation. Within-group differences were compared with the Wilcoxon-Mann-Whitney U test and between-group differences with the Wilcoxon signed-rank test because the sample sizes are too small (just n=6 in each group and n=6 pairs) to allow checking of the assumptions of the unpaired and paired t-tests, respectively. A p-value < 0.05 was considered statistically significant.

Reference

1. Takahashi K, Tanabe K, Ohnuki M, Narita M, Ichisaka T, Tomoda K, Yamanaka S. Induction of pluripotent stem cells from adult human fibroblasts by defined factors. Cell. 2007; 131:861-872.

2. Jaroszeski MJ, Gilbert R, Heller R. Detection and quantitation of cell-cell electrofusion products by flow cytometry. Anal Biochem. 1994; 216:271-275.

3. Teramoto N, Koshino K, Yokoyama I, Miyagawa S, Zeniya T, Hirano Y, Fukuda H, Enmi J, Sawa Y, Knuuti J, Iida H. Experimental pig model of old myocardial infarction with long survival leading to chronic left ventricular dysfunction and remodeling as evaluated by PET. J Nucl Med. 2011; 52:761-768.

4. Teichholz LE, Kreulen T, Herman MV, Gorlin R. Problems in echocardiographic volume determinations: Echocardiographic-angiographic correlations in the presence or absence of asynergy. Am J Cardiol. 1976; 37:7–11.

5. Fukui S, Kitagawa-Sakakida S, Kawamata S, Matsumiya G, Kawaguchi N, Matsuura N, Sawa Y. Therapeutic effect of midkine on cardiac remodeling in infarcted rat hearts. Ann Thorac Surg. 2008; 85:562-570.

6. Zou Y, Liang Y, Gong H, Zhou N, Ma H, Guan A, Sun A, Wang P, Niu Y, Jiang H, Takano H, Toko H, Yao A, Takeshima H, Akazawa H, Shiojima I, Wang Y, Komuro I,

Ge J. Ryanodine receptor type 2 is required for the development of pressure overload-induced cardiac hypertrophy. Hypertension. 2011; 58:1099-1110.

7. Horiguchi K, Kitagawa-Sakakida S, Sawa Y, Li ZZ, Fukushima N, Shirakura R, Matsuda H. Selective chemokine and receptor gene expressions in allografts that develop transplant vasculopathy. J Heart Lung Transplant. 2002; 21:1090-1100.

Mol Cell Biochem (2012) 368:203–214
DOI 10.1007/s11010-012-1361-4

Transplantation of elastin-secreting myoblast sheets improves cardiac function in infarcted rat heart

Ayako Uchinaka · Naomasa Kawaguchi · Yoshinosuke Hamada · Shigeru Miyagawa · Atsuhiro Saito · Seiji Mori · Yoshiki Sawa · Nariaki Matsuura

Received: 15 February 2012 / Accepted: 7 June 2012 / Published online: 21 June 2012

Abstract Myoblast sheet transplantation for cardiac failure is a promising therapy to enhance cardiac function via paracrine mechanism. However, their efficacies of treatment showed a gradual decline. The gene modification of the implanted myoblast is important in improving the long-term results of the treatment. Elastin fiber enhances the extensibility of the infarcted wall and can prevent left ventricular dilation. We therefore hypothesized that the elastin gene modification of the implanted myoblast could strengthen and maintain the long-term improvement effects of cardiac function. In this study, we evaluated long-term follow-up benefits of functional myoblast sheets that secrete elastin in an infarcted model. The animal models were divided into three groups: a group transplanted with nontransfected, wild-type, skeletal myoblast-type sheets (WT-rSkM); group transplanted with myoblast sheets that secreted elastin fragments (ELN-rSkM); and a control group (ligation only). Cardiac function was examined by echocardiography, and cardiac remodeling after infarction was evaluated by histological examination. The cardiac function was significantly improved and the left ventricle end-diastolic dimensions were significantly reduced in the ELN-rSkM group. Histological analysis showed that left ventricular remodeling was attenuated in the ELN-rSkM group and that elastic fiber was formed in the epicardial area of ELN-rSkM group. The functionalization of myoblast sheet by elastin gene transfer showed the long-term improvement of cardiac function. Expressed recombinant elastin fiber prevented the dilation of the left ventricular chamber after myocardial infarction. The functional myoblast sheet transplantation maintained the treatment effect by the paracrine effect of myoblast and the formed recombinant elastin.

Keywords Myocardial infarction · Cell transplantation · Remodeling · Elastin · Gene expression

A. Uchinaka · N. Kawaguchi (✉) · Y. Hamada · S. Mori · N. Matsuura
Department of Molecular pathology, Osaka University Graduate School of Medicine, Division of Health Sciences, 1-7 Yamada-oka, Suita, Osaka 565-0871, Japan
e-mail: kawaguch@sahs.med.osaka-u.ac.jp

S. Miyagawa · Y. Sawa
Department of Cardiovascular Surgery, Osaka University Graduate School of Medicine, Suita, Japan

A. Saito
Medical Center of Translational Research, Osaka University Graduate School of Medicine, Suita, Japan

Introduction

In recent years, myocardial regeneration therapy using cell transplantation has been examined for the treatment of heart failure [1–3]. In the several cell sources such as smooth muscle cells and bone marrow-derived cells, transplantation of skeletal myoblasts have achieved better therapeutic effects [4–6]. The therapeutic effect of the myoblast sheet is considered to be mediated by the production of paracrine effectors that locally stimulate the injured myocardium [7, 8]. However, autologous skeletal myoblast transplantation by means of the injection method has some disadvantages, including the loss of transplanted cells, inadequate survival of grafted cells, and arrhythmogenicity [9, 10]. We therefore investigated a novel cell transplantation technique using cell sheets grown in temperature-responsive dishes [8, 11] as a means of overcoming these problems. We have previously shown that transplantation of autologous skeletal myoblast sheets is

superior to direct myocardial injection in cell therapy of heart failure in studies on both small and large animals [12–14]. Furthermore, beneficial results of the implantation of a layered myoblast sheet in comparison with a single-layered sheet included a greater improvement in cardiac function, fewer fibrosis, and less hypertrophy [15].And, when layered myoblast sheets were transplanted onto the infarcted area, the amount of elastic fiber increased in the implanted area with expression of tropoelastin mRNA. The relative expression of rat tropoelastin mRNA increased in a dose-dependent fashion [15]. We therefore hypothesize that the expression of elastin is a contributory factor in the therapeutic effects of myoblast sheets and that the overexpression of elastin could strengthen these effects.

When we followed up the cardiac function after myoblast sheet transplantation until 8 weeks after sheet transplantation, the efficacies of the sheet transplantation showed a gradual decline. The modification of the implanted myoblast is very important in improving the long-term results of the treatment. In curing cardiac disease, the necrotic myocardium is replaced by collagen fiber, and elasticity is lost in the scarred area. As a result, the diastolic performance of the left ventricle (LV) declines with time [16, 17]. Therefore, we hypothesized that elastin secreted from the implanted myoblast sheets might generate elasticity in the infarcted area. Additionally, by transplantation of the sheets to the epicardium, we hoped that a layer of elastic fiber would be formed and inhibit dilatation of the LV chamber, conferring a guard ring effect. Because the lifespan of elastin fibers is in the region of years, the cardiac function might be stabilized in the long term. At present, myocardial regeneration therapy using cell transplantation combined with elastin is hardly ever performed in the case of serious heart failure, and approaches to therapy of cardiac disease with elastin have not been reported besides the reports by Mizuno et al. Mizuno and co-workers reported that injection of elastin gene-transfected COS7 cells into an infarcted heart improved its performance[18, 19]. The COS7 cell is an endothelial cell from the African green monkey kidney, and endothelial cells alone do not improve the function of the LV after myocardial damage. Because we used myoblasts, which can themselves affect cardiac function and remodeling, additional therapeutic effects might be expected. We have expected that the paracrine function by myoblast will have a curative effect in the early stage, and the guard ring function of the recombinant elastin will inhibit the LV chamber dilation in the late stage.

In the present study, we constructed functional skeletal myoblast sheets that secrete elastin and examined their effects in improving cardiac function and the remodeling in rats with myocardial infarction (MI).

Materials and methods

Isolation of skeletal myoblasts

Myoblasts were isolated from the skeletal muscle of the tibialis anterior from three-week-old male Lewis rats. After the removal of connective tissues, such as tendons and fibrous tissue, the muscles were minced and enzymatically dissociated with 0.2 % collagenase type II (Worthington Biochemical Corp., Lakewood, NJ, USA) and trypsin for 30 min at 37 °C. The enzymatic reaction was arrested by addition of Dulbecco's modified Eagle's medium (DMEM) (Nihonseiyaku, Tokyo, Japan) containing 20 % fetal bovine serum (FBS) (Biowest, Miami, FL, USA), and the cells were collected by centrifugation. The cells were suspended in culture medium composed of DMEM with 20 % FBS and 1 % antibiotic–antimycotic solution (Invitrogen Life Technologies). After being pre-plated twice, nonadherent cells were then plated on a Matrigel (Becton–Dickinson Bioscience)-coated dish and incubated at 37 °C, 5 % CO_2. The purity of the culture was evaluated by immunofluorescence imaging. The isolated cells fixed with 4 % paraformaldehyde were incubated with anti-desmin antibody (Sigma, St. Louis, MO, USA) and followed by incubation with fluorescein isothiocyanate [FITC; 2-(3,6-dihydroxy-9H-xanthen-9-yl)-5-isothiocyanato-benzoic acid] conjugated anti-rabbit secondary antibody (GE Healthcare, Piscataway, NJ, USA). The nuclei were stained with 4′,6-diamino-2-phenylindole (DAPI; Invitrogen Life Technologies) and the fluorescent signals were detected by fluorescence microscopy (ECLIPSE E600, Nikon, Tokyo, Japan).

Animal ethics

This animal experiment was approved by the Animal Care Committee of Osaka University graduate school of medicine. Humane animal care was used in compliance with the Principals of Laboratory Animal Care formulated by the National Society for Medical Research, and the Guide for the Care and Use of Laboratory Animals prepared by the Institute of Laboratory Animal Resource and published by the National Institute of Health (NIH publication No.85–23, revised 1996).

Animal model

Eight-week old female F344/NJcl-rnu/rnu rats were used as recipients. The rats were anesthetized with isoflurane (2 %, 0.2 ml/min) by inhalation. They were then intubated, and respirator served to maintain ventilation during surgery. The adequacy of anesthesia was monitored by electrocardiogram and pulse rate. MI was produced by ligation of the

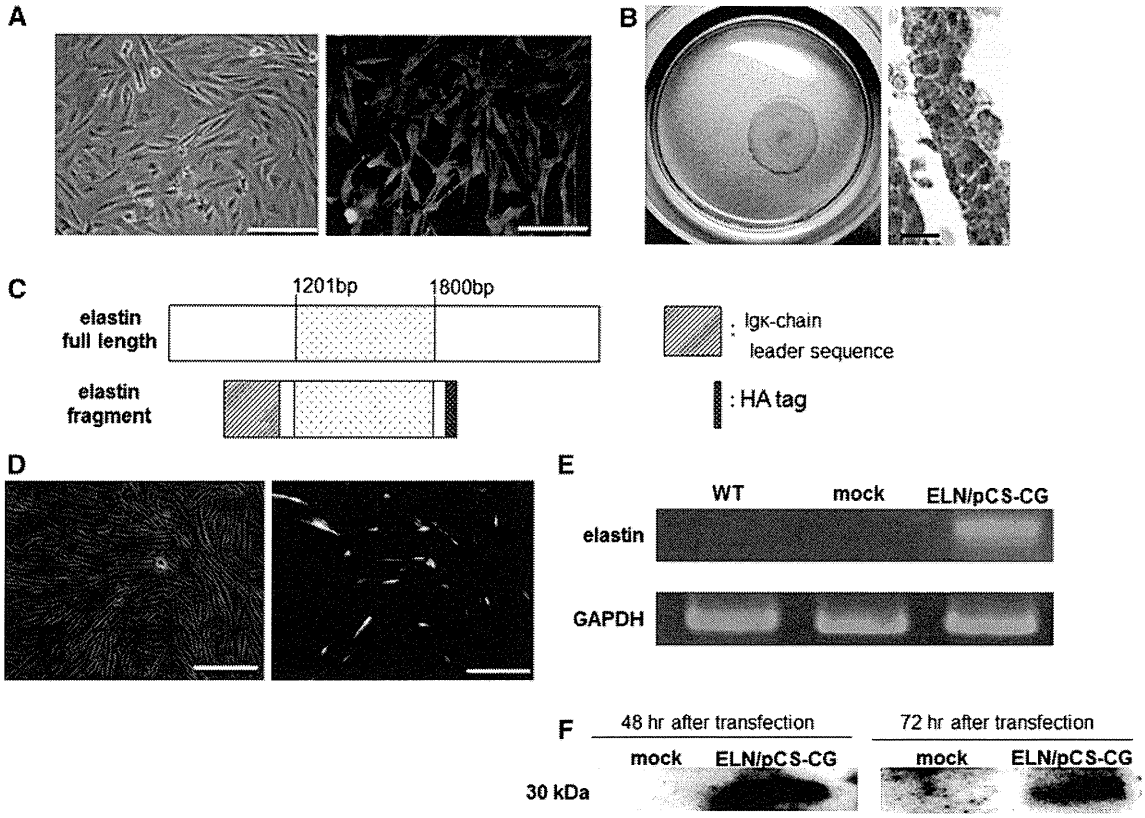

Fig. 1 Characteristics of isolated myoblasts and expression of elastin in isolated myoblasts. **a** Isolated skeletal myoblasts (passage 2) (*left-hand side*) and its immunofluorescent staining (*right-hand side*) (*green* desmin, *blue* nucleus *scale bar* 100 μm). High-purity skeletal myoblasts can therefore be isolated. **b** The rat skeletal myoblast (rSkM) sheet (*left*). Staining by hematoxylin and eosin of a cross section of the rSkM sheet (*right*, *scale bar* 50 μm). **c** View showing the frame format of the constructed rat tropoelastin gene. **d** Determination of lentiviral transduction efficiency (*scale bar* 100 μm). **e**, **f** Assessment of expression of the recombinant elastin by RT-PCR and western blotting. The secreted recombinant elastin protein was detected in the culture medium of rSkM cells infected with ELN/pCS-CG, whereas no elastin expression was detected in control cells

left anterior descending coronary artery (LAD). When the baseline cardiac function was measured by echocardiography two weeks after the ligation, we monitored the depression of the left ventricular anterior wall movement. And, at the time of sheet transplantation, we macroscopically confirmed the scar area which spread from ligated portion toward cardiac apex, and implanted the myoblast sheets on the scar region without use of suture. The rats were divided into three groups: (1) a WT-rSkM group (implanted with three nontransfected wild-type myoblast sheets, $n = 6$), (2) an ELN-rSkM group (implanted with three myoblast sheets that secreted elastin fragments, $n = 8$), and (3) a control group (re-opened the chest at 2 weeks when other two groups were implanted with myoblast sheets, $n = 6$). The implanted sheets adhere to myocardium immediately and don't fall off after closing the chest because the cell sheets maintain the cell–cell and cell-extracellular matrix (ECM) adhesion. After detachment from the temperature-responsive dish, each sheet was picked up individually and applied to surface of the heart. So that the sheet could be spread, the folded areas were gently stoked with wet, round tip forceps. After confirmation of the adherence of the implanted sheets, subsequent sheets were applied by the same technique.

Elastin overexpression and transfection

Lentiviral vector which includes the cDNA of the fragment (from 1,201 to 1,800 bp) of rat tropoelastin (ELN/pCS-CG) was constructed (Fig. 1c). And the isolated rSkM were transfected with incubation for 48 h in the presence of ELN/pCS-CG and 8 μg/ml polybrene (Sigma). Expression of the recombinant elastin gene was examined by RT-PCR and Western blotting after 5 days.

Reverse transcription-polymerase chain reaction assay

After 5 days of transduction, the cells were lysed with Sepasol (Nacalai Tesque, Kyoto, Japan), and the total RNA was isolated. Glyceraldehyde 3-phosphate dehydrogenase (GAPDH) was used as an internal control.

The following primer sequences were used for PCR: elastin fragment (333 bp): 5′-GGTGCACTGCCAGGTGC AGTACCA-3′ (forward) and 5′-AGCGTAATCTGGAAC ATCGTATGG-3′ (reverse) rat GAPDH (393 bp): 5′-ACT GGCGTCTTCACCACCAT-3′ (forward) and 5′-AGTGA GCTTCCCGTTCAGCT-3′(reverse)

Western blotting assay

The culture medium was collected and centrifuged, and supernatants were used for the assays. Each sample was subjected to electrophoresis on polyacrylamide gels and then electro transferred to a polyvinylidene fluoride transfer membrane (Millipore, Billerica, MA, USA). After blocking (5 % nonfat milk), the membrane was probed with a primary antibody against HA tag (Santa Cruz Biotechnology, California, USA). The membranes were incubated with anti-rabbit IgG-linked horseradish peroxidase (GE Health care) and then exposed to SuperSignal West Femto (Thermo Fisher Scientific Inc, Waltham, MA, USA).

Sheet production

Four days after lentivirus transduction, 3×10^6 infected myoblasts were placed on a 35-mm temperature-responsive culture dish (UpCell; Cellsheed, Tokyo, Japan) and incubated. After 16 h, the cell sheets were detached at room temperature for 30 min (Fig. 1b).

Measurement of cardiac function

The cardiac function of the treated rats was monitored by echocardiography 2, 4, 6, and 8 weeks after sheet implantation. The measurements were performed by using a SONOS 5500 sonograph (Agilent Technologies, Palo Alto, Calif) with a 12-MHz transducer. The rats were anesthetized with isoflurane (2 %, 0.2 ml/min) by inhalation, as mentioned above. The hearts were visualized as short-axis two-dimensional images at the level of the papillary muscles. The LV-end systolic area, the LV-end diastolic area, and the LV dimensions at end-systole and end-diastole (LVIDd and LVIDs, respectively) were determined. On the basis of these results, the ejection fraction (EF), fractional shortening (FS), end-diastolic volume (EDV), and end-systolic volume (ESV) were calculated as follows.

(1) $\text{LVEF}\ (\%) = (\text{LVDd}^3 - \text{LVDs}^3)/\text{LVDd}^3 \times 100\ (\%)$.
(2) $\text{LV}\ \%\ \text{FS} = [(\text{LVDd} - \text{LVDs})/\text{LVDd}] \times 100\ (\%)$.
(3) $\text{EDV} = \text{LVIDd}^3 \times (0.98 \times \text{LVIDd} + 5.90)\ (\text{ml})$.
(4) $\text{ESV} = \text{LVIDs}^3 \times (1.14 \times \text{LVIDs} + 4.18)\ (\text{ml})$.

Heart weight/body weight ratio

The rats' body weights were measured 8 weeks after sheet transplantation. And then, the rats were anesthetized with intraperitoneal pentobarbital (300 mg/kg) and heparin (150 U), and their hearts were rapidly removed. The weights of the removed hearts were also measured and the ratio of the heart weight (mg) to the body weight (g) (HW/BW) was calculated.

Histological analyses

LV myocardium species were obtained 8 weeks after sheet implantation. The fixed sample was embedded in paraffin. The LV chamber diameter and the anterior wall thickness were measured for sections stained with Hematoxylin–Eosin (HE). Infarcted wall thickness, posterior wall thickness, and LV chamber diameter were measured with the scale loupe. Sirius red stain was used to detect the fibrosis. The fibrosis was evaluated from the fibrotic ratio in the infarct border region at a magnification of 200×. Periodic acid–Schiff staining for cardiomyocyte hypertrophy was also performed. Cardiomyocytes ($n = 100$) at 400× magnification were randomly selected in border and remote area of the infarct, and their minor axes across the nucleus were measured. To label vascular endothelial cells so that blood vessels could be counted, we performed immunohistochemical staining for Von Willebrand factor antigen. Paraffin sections were deparaffinized in xylene, dehydrated in graded ethanol mixtures, and processed for antigen retrieval by autoclaving in 0.01-M citrate buffer. Endogenous peroxidase was blocked by immersing the sections in methanol containing 3 % hydrogen peroxide. After blocking with 5 % BSA, the sections were incubated with primary antibody against Von Willebrand Factor (rabbit-polyclonal; DAKO, Glostrup, Denmark). The sections were incubated with a biotinylated anti-rabbit IgG antibody (DAKO) and further incubated with a peroxidase-conjugated streptavidin (GE Health Care). Visualization was performed using biphenyl-3,3′,4,4′-tetramine (DAB) solution (Sigma). Twenty different fields at 400× magnification were randomly selected, and the number of the stained vascular endothelial cells in each field was counted under a light microscope. The distribution of elastin fibers was evaluated by means of Victoria blue-HE staining or elastica van Gieson staining.

Expression of elastin and matrix metalloproteinase in myocardial tissue

The samples of myocardial tissue removed 8 weeks after sheet transplantation were divided into infarction, border, and remote areas. Each sample was homogenized in SDS

buffer and centrifuged, and the supernatants were used for assays by Western blotting, as previously described. The primary antibodies used were rabbit polyclonal anti-elastin (Acris Antibodies GmbH, Herford, Germany), rabbit polyclonal anti-matrix metalloproteinase 1 (anti-MMP-1) (LifeSpan Biosciences Inc., Seattle, WA, USA), mouse monoclonal anti-matrix metalloproteinase 2 (anti-MMP-2) (Daiichi Fine Chemical Co., Ltd., Toyama, Japan), and mouse monoclonal anti-muscle actin (Dako). We quantified the density of the bands of elastin, MMP-1, and MMP-2 using α-tubulin of each lane as a standard.

Statistical analyses

Data are presented as the mean ± standard error of mean (SEM). The cardiac function was analyzed by repeated measurement ANOVA for differences across the whole time course and one-way ANOVA, whereas the Tukey–Kramer post hoc test was used to examine for significant differences at each time point.

To assess the significance of the differences between individual groups for other data, statistical comparisons were performed by an unpaired Student's *t* test. A value of $P < 0.05$ was considered statistically significant.

Results

Isolation of rat skeletal myoblasts

To confirm that the isolated cells from the skeletal muscle were myoblasts, we performed immunofluorescent staining with anti-Desmin antibody. Fluorescence microscopy studies showed that more than 80 % of the isolated cells were desmin-positive (Fig. 1a). High-purity skeletal myoblasts can therefore be isolated.

mRNA expression and elastin secretion in rat skeletal myoblasts

The efficiency of infection of the rSkM was >70 % (Fig. 1d). The expression of elastin mRNA was recognized in rSkM infected with ELN/pCS-CG (Fig. 1e), whereas expression of elastin was not detected in noninfected rSkM (WT) or control cells infected with the empty vector (mock). The secreted recombinant elastin protein was detected in the culture medium of rSkM cells infected with ELN/pCS-CG, whereas no elastin expression was detected in the control cells (Fig. 1f).

Elastin-expressing myoblast sheets enhance ventricular function after MI

There was no difference in echocardiographic parameters such as LVEF or %FS between the groups before sheet transplantation. Echocardiography showed a significant improvement in LVEF and %FS in the WT-rSkM and ELN-rSkM groups in comparison with the control group 2, 4, 6, or 8 weeks after implantation ($P < 0.01$). In addition, the values of LVEF and %FS in the ELN-rSkM group 2, 6, and 8 weeks after implantation were significantly improved in comparison with that of the WT-rSkM group (2 and 6 weeks; $P < 0.05$; 8 weeks; $P < 0.01$) (Figs. 2a, b).

The evaluation of LVIDd and LVIDs over time showed the inhibition of dilation in all measure points in the ELN-rSkM group relative to the control and WT-rSkM groups. And, especially at late points, 6 and 8 weeks after implantation, they were significantly attenuated in the ELN-rSkM group compared with the control group (LVIDd: 8 weeks $P < 0.05$, LVIDs: 6 weeks $P < 0.05$, 8 weeks $P < 0.01$) (Table 1). The values of EDV and ESV in the ELN-rSkM group were also smaller than the control and WT-rSkM groups in all measure points. The

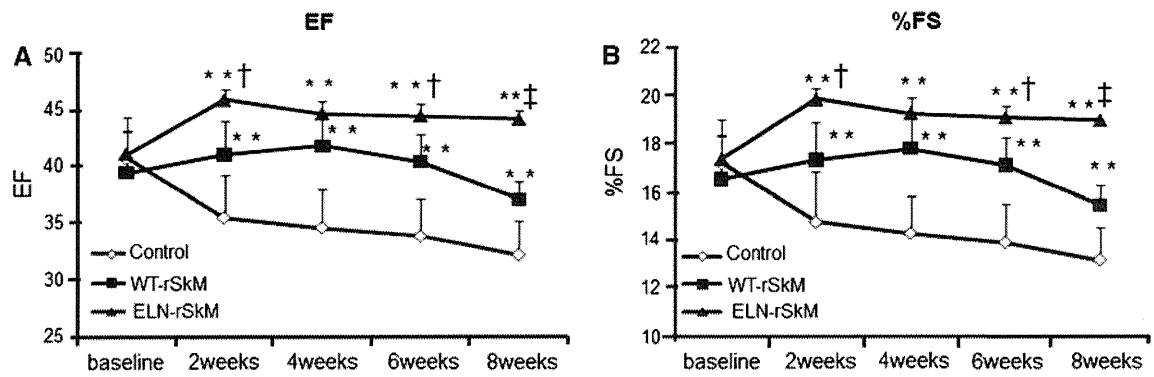

Fig. 2 Left ventricular function after myoblast sheet transplantation by echocardiography (**a** *EF* ejection fraction, **b** *% FS %* fractional shortening) Echocardiography showed a significant improvement in LVEF and % FS in the WT-rSkM and ELN-rSkM groups in comparison with the control group 2, 4, 6, or 8 weeks after implantation. In addition, the values of LVEF and %FS in the ELN-rSkM group 2, 6, and 8 weeks after implantation were significantly improved in comparison with that of the WT-rSkM group $^{**}P < 0.01$ versus control. †$P < 0.05$, ‡$P < 0.01$ versus WT-rSkM

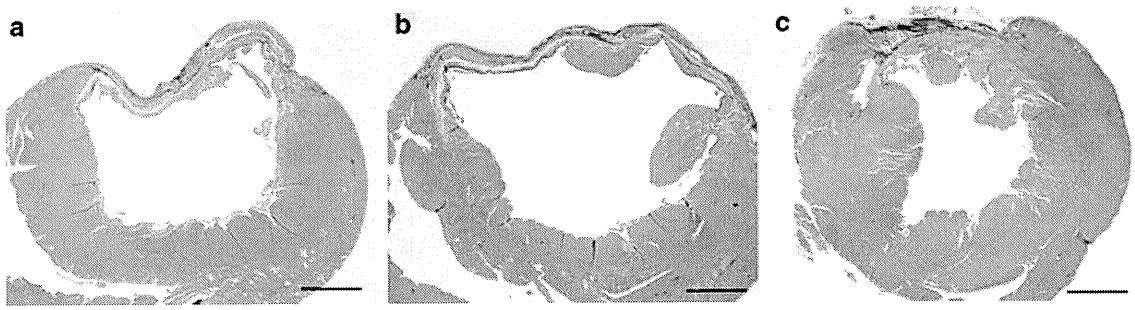

Fig. 3 Victoria blue-HE stained section of LV **a** control, **b** WT-rSkM, **c** ELN-rSkM (×10, *scale bar* 1,000 μm, *blue*: elastic fiber). The occurrence of thinning of the infarcted wall in the control group and the WT-rSkM group, whereas its thickness was maintained in the ELN-rSkM group

Table 1 The assessments of LVIDd, LVIDs, EDV, and ESV over time by echocardiography

	Baseline	2 weeks	4 weeks	6 weeks	8 weeks
LVIDd					
Control	0.73 ± 0.08	0.77 ± 0.07	0.81 ± 0.05	0.86 ± 0.05	0.88 ± 0.04
WT-rSkM	0.72 ± 0.08	0.77 ± 0.03	0.79 ± 0.04	0.83 ± 0.05	0.85 ± 0.04
ELN-rSkM	0.71 ± 0.09	0.73 ± 0.08	0.77 ± 0.06	0.80 ± 0.05	0.80 ± 0.06*
LVIDs					
Control	0.60 ± 0.06	0.65 ± 0.06	0.69 ± 0.04	0.74 ± 0.05	0.76 ± 0.04
WT-rSkM	0.61 ± 0.07	0.63 ± 0.03	0.67 ± 0.05	0.70 ± 0.04	0.72 ± 0.03
ELN-rSkM	0.59 ± 0.07	0.59 ± 0.07	0.63 ± 0.05	0.67 ± 0.05*	0.67 ± 0.06**
EDV					
Control	2.60 ± 0.78	3.05 ± 0.91	3.59 ± 0.66	4.29 ± 0.70	4.57 ± 0.59
WT-rSkM	2.54 ± 0.74	3.11 ± 0.32	3.33 ± 0.54	3.86 ± 0.71	4.07 ± 0.61
ELN-rSkM	2.45 ± 0.84	2.68 ± 0.92	3.19 ± 0.74	3.48 ± 0.73	3.50 ± 0.86*
ESV					
Control	1.07 ± 0.30	1.40 ± 0.38	1.67 ± 0.31	2.06 ± 0.44	2.23 ± 0.35
WT-rSkM	1.13 ± 0.32	1.25 ± 0.16	1.50 ± 0.34	1.69 ± 0.30	1.86 ± 0.26
ELN-rSkM	1.01 ± 0.35	1.01 ± 0.37	1.26 ± 0.30	1.49 ± 0.33*	1.50 ± 0.32**

* $P < 0.05$, ** $P < 0.01$ versus control of each measure point

enlargement of EDV was also significantly attenuated in the ELN-rSkM group compared with the control group eight weeks after implantation ($P < 0.05$) (Table 1). The ESV showed a significant decrease in the ELN-rSkM group compared with the control group at both six and eight weeks after implantation (6 weeks $P < 0.05$, 8 weeks $P < 0.01$) (Table 1).

The decline of heart weight/body weight ratio

To evaluate the degree of cardiac hypertrophy, we used the HW/BW ratio as an indicator. HW/BW showed a significant decrease in the ELN-rSkM group compared with the control and WT-rSkM groups ($P < 0.01$ versus control, $P < 0.05$ versus WT-rSkM) (Table 2).

Myoblast sheets secreting elastin exert therapeutic effects on injured myocardium

Victoria blue-HE stained sections demonstrated the occurrence of thinning of the infarcted wall in the control group and the WT-rSkM group, whereas its thickness was maintained in the ELN-rSkM group (Fig. 3; Table 3). A statistical analysis showed that the diameter of the LV chamber was smaller in the ELN-rSkM than in the control or WT-rSkM groups ($P < 0.05$) (Table 3), and that the thickness of the infarcted wall in the ELN-rSkM group was significantly greater than that in the control or WT-rSkM groups ($P < 0.01$) (Table 3). The values of the LV chamber diameter/posterior wall thickness were significantly decreased in the ELN-rSkM group compared with the control group and WT-rSkM group ($P < 0.01$) (Table 3).

Table 2 The heart weight/body weight (HW/BW) ratio at 8 weeks after sheet transplantation

	Body weight (BW) (g)	Heart weight (HW) (mg)	HW/BW
Control	184.97 ± 7.94	763.33 ± 5.53	4.13 ± 0.17
WT-rSkM	184.19 ± 9.01	705.00 ± 5.61	3.83 ± 0.34*
ELN-rSkM	190.88 ± 8.08	677.50 ± 4.77	3.55 ± 0.20**†

* $P < 0.05$, ** $P < 0.01$ versus control. † $P < 0.05$ versus WT-rSkM

Table 3 The thickness of infarcted wall and posterior wall and LV chamber

	Control	WT-rSkM	ELN-rSkM
LV chamber diameter (mm)	4.55 ± 0.52	4.40 ± 0.45	3.81 ± 0.52*†
Infarcted wall thickness (mm)	0.47 ± 0.13	0.49 ± 0.09	0.63 ± 0.13
Posterior wall thickness (mm)	1.82 ± 0.19	1.75 ± 0.27	1.78 ± 0.19
% Anterior wall thickness	26.40 ± 2.96	27.76 ± 2.08	35.88. ± 2.29**‡
LV chamber diameter/ posterior wall thickness	2.50 ± 0.16	2.51 ± 0.18	2.14 ± 0.16**‡

% Anterior wall thickness = infarcted wall thickness/posterior wall thickness ×100 * $P < 0.05$, ** $P < 0.05$, ‡ $P < 0.01$ versus control, † $P < 0.05$, ‡ $P < 0.01$ versus WT-rSkM

There were no significant differences between the control and WT-rSkM groups on these indexes.

In the border area, staining with picrosirius red showed the presence of a significant reduction of fibrosis in the ELN-rSkM group in comparison with the control and WT-rSkM groups ($P < 0.01$) [Figs. 4A(a)–(c), B(a)]. Periodic acid–Schiff staining showed that the diameters of the cardiomyocytes in the ELN-rSkM group were significantly smaller than those in the control or WT-rSkM groups ($P < 0.01$) [Figs. 4A(d)–(f), B(b)].

The vascular density was significantly increased in the WT-rSkM and ELN-rSkM groups compared with the control group ($P < 0.01$), but there were no significant differences between the WT-rSkM and ELN-rSkM groups [Figs. 4A(g)–(i), B(c)]. Fibrosis, cell size, and vascular density were not different in the remote area among three groups.

Increase in the distribution of elastic fibers in epicardial area of implanted area

Victoria blue-HE and Elastica van Gieson stained sections showed that the numbers of elastic fibers were increased in the ELN-rSkM group [Figs. 3c, 5A(c), B(f)]. Recombinant elastin was widely detected throughout the scar area and border zone in the epicardial area of the ELN-rSkM group, and when it was examined at a higher magnification (×200), it was found to form long wavy structures [Fig. 5B(f)]. The layers of formed elastin fiber would have showed the guard ring effect and depressed the dilation of LV chamber. In contrast, it was scarce in the control and WT-rSkM groups [Figs. 3a, b, 5A(a), (b), B(d), (e)].

The alteration of expression of matrix metalloproteinase 1 and 2 by recombinant elastin

The expression of recombinant elastin was only recognized in infarcted areas of the ELN-rSkM group [Fig. 6A, B(a)]. The expression of MMP-1 was increased in border areas of the ELN-rSkM group compared with that in the control and WT-rSkM groups [Fig. 6A, B(b)]. In the control group, expression of MMP-2 was detected in infarcted, border, and remote areas, whereas in the WT-rSkM group, although it was detected in the infarcted area, there was little expression in border and remote areas. In the ELN-rSkM group, expression of MMP-2 was barely detectable in any area [Fig. 6A, B(c)].

Discussion

Elastin is a major insoluble ECM component. The elastic fiber provides elasticity and extensibility to tissue. Elastin fibers consist of a core of tropoelastin together with crosslinked proteins, including microfibril and fibrillin [20–24]. Elastin contains two major repeated peptide sequences: the pentapeptide Gly-Val-Gly-Val-Pro (GVGVP) and the hexapeptide Val-Gly-Val-Ala-Pro-Gly (VGVAPG). GVGVP has elasticity properties, whereas VGVAPG lacks elasticity, but does induce proliferation and migration of fibroblasts and smooth muscle cells [25–28]. It would have been preferable to express the full length of the elastin gene, but rat tropoelastin cDNA (2,595 bp) is a difficult protein to express, and when we attempted to express the full-length protein, we were unable to do so. We therefore chose a 600-bp (1,201–1,800 bps) segment of the rat tropoelastin. The elastic and resilient properties of elastin are located within this fragment [20].

The cell sheets are generated on and removed from special dishes that are coated with a temperature-responsive polymer, poly [*N*-isopropylacrylamide], that changes from hydrophobic to hydrophilic when the temperature is lowered without destroying the cell–cell or cell-ECM adhesions in the cell sheet. Typical cell harvests by means of enzymatic digestion therefore result in the disruption of both adhesive proteins and membrane receptors. The

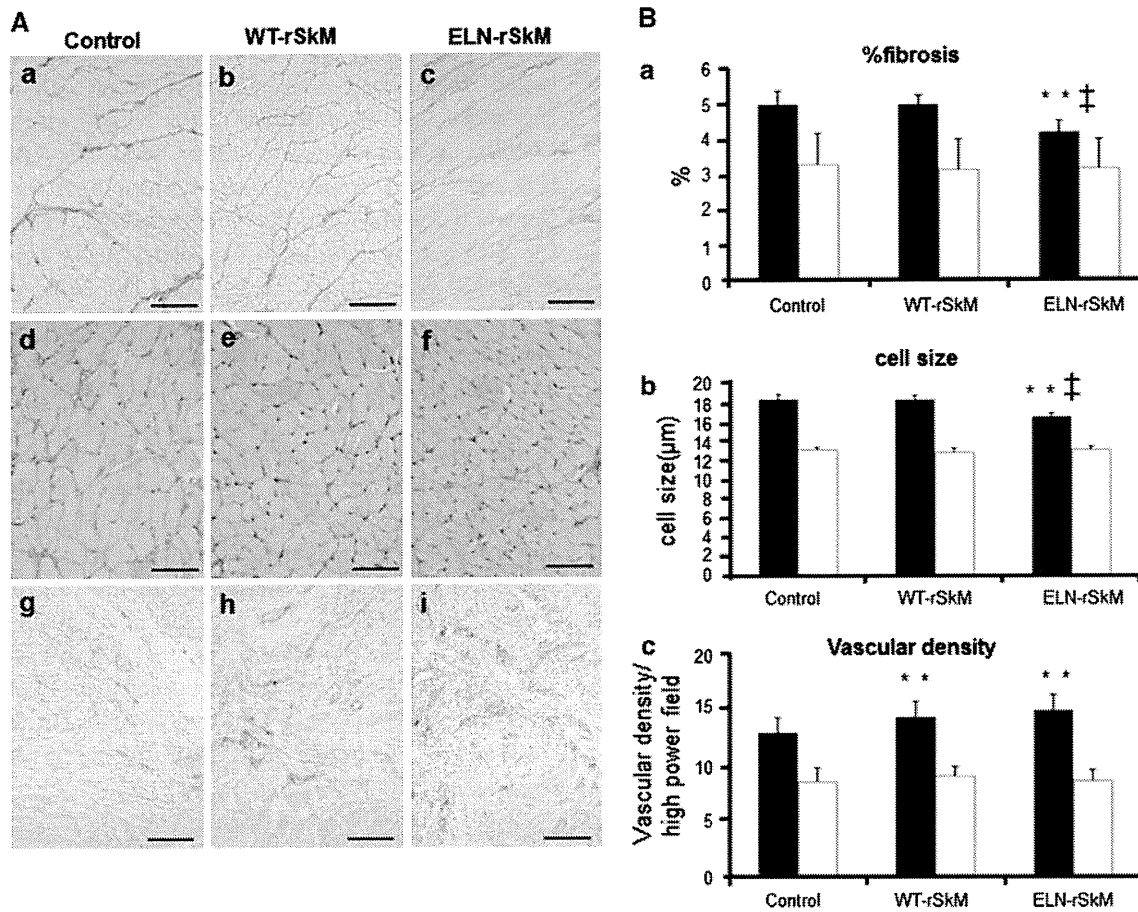

Fig. 4 Histological evaluations of LV remodeling after infarction. **A** Sirius-red stained myocardium of the infarcted border zone *a* control, *b* WT-rSkM *c* ELN-rSkM (×200, *scale bar* 100 μm); periodic acid–Schiff staining of cardiomyocyte of infarcted border zone: *d* control, *e* WT-rSkM, *f* ELN-rSkM (×400, *scale bar* 50 μm); and section of infarcted border zone stained with antibody against Von Willebrand factor: *g* control, *h* WT-rSkM, *i* ELN-rSkM (×200, *scale bar* 100 μm). **B** Quantitative estimation of histological study results: *a* %fibrosis, *b* cell size, *c* vascular density. Histological analysis showed that left ventricular remodeling such as fibrosis and cardiomyocyte hypertrophy were attenuated in the ELN-rSkM group compared with the control and WT-rSkm groups. $^{**}P < 0.01$ versus control. $\dagger P < 0.05$, $\ddagger P < 0.01$ versus WT-rSkM. *Filled bar* border area, *bar* remote area

greatest advantage of this technique is that the sheet is made only of cells, and the cells produce the ECM without requiring an artificial scaffold. The myoblast sheet has a high ability to integrate with area of infarction through the adhesion factors, such as integrin$\alpha 7\beta 1$ and α-dystroglycan, which is expressing on the surface of myoblasts and therefore doesn't fall off after closing the chest.

In this study, we treated hearts, in which MI had been previously induced, by implantation of myoblast sheets that secreted elastin fragments, and we observed continuous improvements in cardiac function and in attenuation of cardiac remodeling. Histological assessment of the ELN-rSkM group showed that elastic fiber was present in both the scarred area and in border zones, whereas this effect was not observed in the control group or the WT-rSkM group. So the accumulation of elastin fibers would be the result of construction of tropoelastin secreted from the transplanted myoblasts.

The dramatic improvements in the left ventricular diastolic and systolic performance in the ELN-rSkM group might be attributable to the formation of elastin fibers in the infarcted region. Accumulation of elastin fibers improved the left ventricular wall movement. The assessments of LVIDd and LVIDs over time showed the continuous depression of dilation of inside diameter in ELN-rSkM group, especially at late points, 6 and 8 weeks after sheet implantation. It is especially noteworthy that the LVIDd in the ELN-rSkM were significantly attenuated 8 weeks after sheet implantation. The myoblast sheets were transplanted into the epicardium and the layers of elastic fiber should have formed epicardial area. Therefore, their guard ring effects might have significantly prevented the outward dilation of the LV chamber in the late stage. And the values of the LV chamber diameter/posterior wall thickness in the ELN-rSkM were significantly smaller than the control and WT-rSkM.

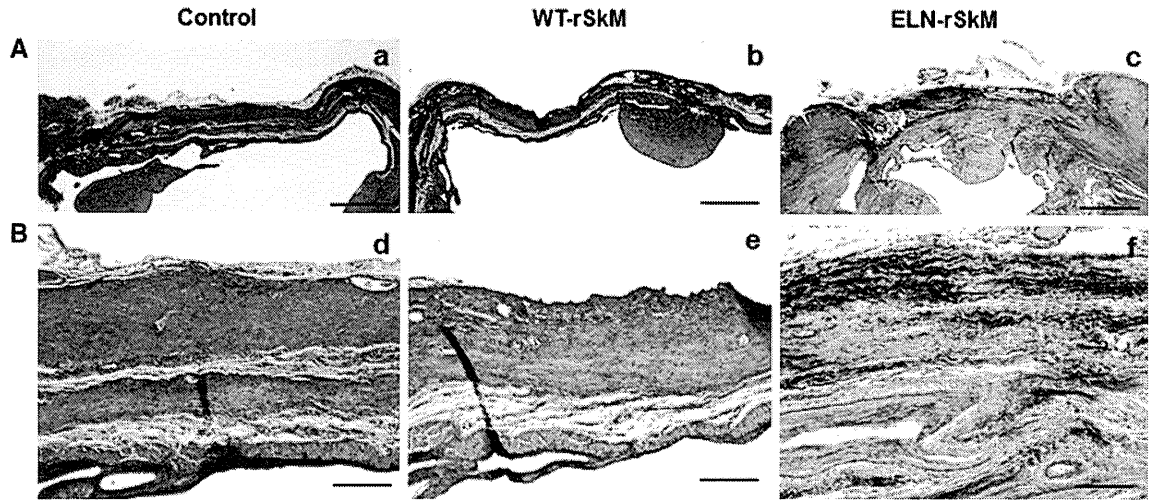

Fig. 5 Elastin distributions in the infarcted area by elastica van Gieson staining and immunohistochemical staining using an antibody against elastin [**A** (*a* control, *b* WT-rSkM, *c* ELN-rSkM, *a–c*, ×20, *scale bar* 500 μm), **B** (*d* control, *e* WT-rSkM, *f* ELN-rSkM, *d–f* ×200, *scale bar* 100 μm)]. Recombinant elastin was widely detected throughout the scar area and border zone in the epicardial area of the ELN-rSkM group

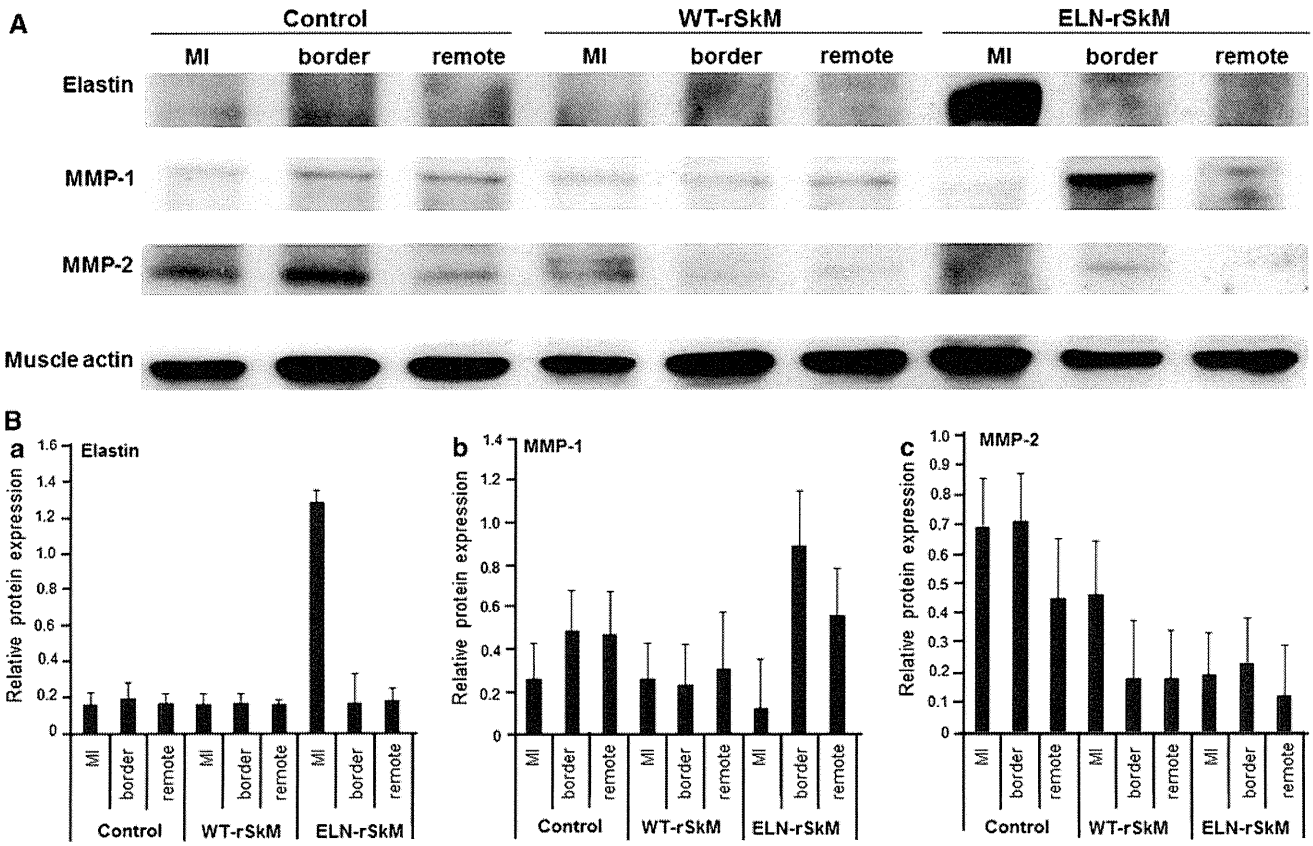

Fig. 6 Expression of elastin, matrix metalloproteinase 1 (MMP-1), and matrix metalloproteinase 2 (MMP-2) examined by western blotting. **A** A representative result of Elastin, MMP-1, and MMP-2 protein expression. **B** Quantitation of western blotting of Elastin, MMP-1, and MMP-2 expression normalized by the corresponding muscle actin expressing levels. *a* Elastin, *b* MMP-1, *c* MMP-2 recombinant elastin was only recognized in infarcted areas of the ELN-rSkM group. The expression of MMP-1 was increased in border areas of the ELN-rSkM group, and the expression of MMP-2 was barely detectable in any area of the ELN-rSkM group compared with that in the control and WT-rSkM groups

Most of the transplanted myoblasts drop out until 4 weeks after sheet transplantation. As a result, cardiac functions such as EF and %FS in the WT-rSkM group was markedly depressed 4 weeks after sheet transplantation. In contrast, because the lifespan of elastin fibers can be measured in years, the elastin fiber that was formed remained after dropout of the transplanted cells and it produced a long-term improvement in cardiac function and attenuation of remodeling. The early therapeutic effects after elastin-secreted myoblast sheets implantation would have been resulted from paracrine growth factors such as VEGF and HGF by myoblasts transplantation, and the late effects have been caused by the guard ring function of the formed elastin fibers.

Additionally, owing to the widespread distribution of recombinant elastin fibers in the border zone, adverse impacts on the uninjured myocardium and their exercise quantity were reduced, and consequently, cardiac remodeling processes, such as fibrosis and cardiomyocyte hypertrophy, were attenuated.

Our study would have been significantly strengthened if we had a longer follow-up period. However, a previous study [15] has shown that the cardiac functions such as EF and %FS have been markedly depressed between 4 and 8 weeks after autologous myoblast sheet transplantation. Therefore, in the present study, we have assessed the cardiac function and histological change such as left ventricular remodeling and deposition of elastic fiber over time up to 8 weeks after sheet implantation.

The ECM exerts an influence on cellular movement and cross-interactions, and elastin is a major structural component of the extracellular matrix. The ratio of collagen to elastin in tissue is involved in a variety of clinical conditions, and both MMP and tissue inhibitor of metalloproteinase (TIMP) modulate this ratio. In curing ischemic cardiac disease, the necrotic myocardium is replaced by collagen fiber, especially type I and type III collagen, and elasticity is lost in the scarred area. There are also a few reports that the elastin-derived hexapeptide VGVAPG stimulates the expression of MMP-1 [29–31]. In the present study, we have shown that an increase in MMP-1 expression occurs in the infarcted area of the ELN-rSkM group at 8 weeks after sheet transplantation. This suggests that the recombinant elastin secreted from the myoblasts increased the expression of MMP-1. Increased expression of MMP-1, which mainly decomposes collagen types I and III, inhibits fibrosis and improves cardiac function [32]. The depression of fibrosis in the ELN-rSkM group could, therefore, be due to an increase in MMP-1 expression by recombinant elastin and upregulation of collagen degradation by MMP-1. Furthermore, in cardiac infarction, the degradation products of collagen, laminin, and fibronectin generated by the activity of MMP-2 stimulate macrophage migration in the infarcted myocardium [33]. The macrophages that migrate into the infarcted tissue are involved in inflammation and in the healing process as a result of their phagocytosis function, promoting cardiac fibrosis and regulating LV remodeling [34]. Furthermore, inhibition of MMP2 activity suppresses LV remodeling after infarction and improves the survival rate after an acute MI. In this study, the levels of expression of MMP-2 in the ELN-rSkM group were decreased in comparison with those in the control group and the WT-rSkM group 8 weeks after implantation. The change in expression levels of MMP-2 by recombinant elastin might therefore repress LV remodeling resulting from ECM degradation of MMP-2. The newly formed elastin fibers might themselves alter the composition of the ECM and affect the expression of MMPs, resulting in inhibition of remodeling of the infarcted heart.

Previous researchers have demonstrated that cardiac disease therapy with myoblast sheets can effect improvements in cardiac function. This study identified elastin, produced in a myoblast sheet transfected with the elastin gene, as a factor that might improve the therapeutic effect of myoblast sheets and thereby improve cardiac function in an ongoing manner. However, further research regarding the number of cells and secretion volume is necessary.

Because autologous myoblast sheet transplantation had shown no adverse effects in either preclinical or clinical tests, it seems feasible to adopt this cell transplantation for gene modification. And, the sheet transplantation can be applied to treatment of serious heart failure, and it gives minimal damage to heart muscle compared with cell injections. And, the myoblast sheet transplantation has no worries of tumorigenesis which occurs during the transplantation of embryo-stem cell or induced pluripotent stem cell. Furthermore, the present study used a lentivirus vector to transfect the elastin gene into primary rat skeletal myoblasts. Attempts to use nonviral transfection techniques did not result in expression of elastin protein. We also examined the muscle cell lines such as smooth muscle cell and skeletal muscle cell, as carriers of the elastin gene, but in the cell line, only the virus vector expressed elastin. For clinical applications, further research will be necessary to identify new methods of gene transfection that do not require the use of a virus vector. The past clinical trials indicate the efficacy of myoblast sheet transplantation, and the gene modification of the implanted myoblast is also expected to improve the long-term results of the treatment in the clinical application.

In summary, we have shown that the implantation of elastin-secreting myoblast sheets continuously improved cardiac function, and inhibited cardiac remodeling and dilation of the LV chamber. The functional myoblast sheets to which the elastin gene was transfected improved the long-term treatment result. The recombinant elastin fibers

were formed in the epicardial area so that dilation of the left ventricular chamber after MI was prevented. The early therapeutic effects after elastin-secreted myoblast sheets implantation would have been resulted from paracrine growth factor by transplanted myoblasts, and the late effects have been caused by the guard ring function of the formed elastin fibers. The therapeutic effect of myoblast sheets can be further enhanced by gene therapy using elastin.

Acknowledgments We thank Ibu Matsuzaki and Aya Nakayama for excellent technical assistance.

References

1. Akhyari P, Fedak PWV, Weisel RD, Lee JYJ, Verma S, Mickle DAG, Li RK (2002) Mechanical stretch regimen enhances the formation of bioengineered autologous cardiac muscle grafts. Circulation 106:137–142
2. Hamano K, Nishida M, Hirata K, Mikamo A, Li TS, Harada M, Miura T, Matsuzaki M, Esato K (2001) Local implantation of autologous bone marrow cells for therapeutic angiogenesis in patients with ischemic heart disease. Circ J 65:845–847
3. Tang XL, Rokosh DG, Guo Y, Bolli R (2010) Cardiac progenitor cells and bone marrow-derived very small embryonic-like stem cells for cardiac repair after myocardial infarction. Circ J 74:390–404
4. Chazaud B, Hittinger L, Sonnet C, Champagne S, Le Corvoisier P, Benhaiem-Sigaux N, Unterseeh T, Su J, Merlet P, Rahmouni A, Garot J, Gherardi R, Teiger E (2003) Endoventricular porcine autologous myoblast transplantation can be successfully achieved with minor mechanical cell damage. Cardiovasc Res 58:444–450
5. Pagani FD, DerSimonian H, Zawadzel A, Wetzel K, Edge AS, Jacoby DB (2003) Autologous skeletal myoblast transplanted to ischemia-damaged myocardium in human. J Am Coll Cardiol 41:879–888
6. Premaratne GU, Tambara K, Fujita M, Lin X, Kanemitsu N, Tomita S, Sakaguchi G, Nakajima H, Ikeda T, Komeda M (2006) Repeated implantation is a more effective cell delivery method in skeletal myoblast transplantation for rat myocardial infarction. Circ J 70:1184–1189
7. Memon IA, Sawa Y, Miyagawa S, Taketani S, Matsuda H (2005) Combined autologous cellular cardiomyoplasty with skeletal myoblasts and bone marrow cells in canine hearts for ischemic cardiomyopathy. J Thorac Cardiovasc Surg 130:646–653
8. Memon IA, Sawa Y, Fukushima N, Matsumiya G, Miyagawa S, Taketani S, Sakakida SK, Kondoh H, Aleshin AN, Shimizu T, Okano T, Matsuda H (2005) Repair of impaired myocardium by means of implantation of engineered autologous myoblast sheets. J Thorac Cardiovasc Surg 130:1333–1341
9. Suzuki K, Murtuza B, Fukushima S, Smolenski RT, Varela-Carver A, Coppen SR (2004) Targeted cell delivery into infarcted rat hearts by retrograde intracoronary infusion: distribution, dynamics, and influence on cardiac function. Circulation 110:225–230
10. Fernandes S, Amirault JC, Lande G, Nguyen JM, Forest V, Bignolais O, Lamirault G, Heudes D, Orsonneau JL, Heymann MF, Charpentier F, Lemarchand P (2006) Autologous myoblast transplantation after myocardial infarction increases the inducibility of ventricular arrhythmias. Cardiovasc Res 69:348–358
11. Okano T, Yamada N, Okuhara M, Sakai H, Sakurai Y (1995) Mechanism of cell detachment from temperature-modulated, hydrophilic-hydrophobic polymer surfaces. Biomaterials 16: 297–303
12. Miyagawa S, Sawa Y, Kitabayashi-Sakakida S, Taketani S, Memon IA, Kondoh H (2005) Tissue cardiomyoplasty using bioengineered contractile cardiomyocytes sheets to repair damaged myocardium: their integration with recipient myocardium. Transplantation 80:1586–1595
13. Kondoh H, Sawa Y, Miyagawa S, Sakakida-Kitagawa S, Memon IA, Kawaguchi N, Matsuura N, Shimizu T, Okano T, Matsuda H (2006) Longer preservation of cardiac performance by sheet-shaped myoblast implantation in dilated cardiomyopathic hamsters. Cardiovasc Res 69:466–475
14. Hata H, Matsumiya G, Miyagawa S, Kondoh H, Kawaguchi N, Matsuura N, Shimizu T, Okano T, Matsuda H, Sawa Y (2006) Grafted skeletal myoblast sheets attenuate myocardial remodeling in pacing-induced canine heart failure model. J Thorac Cardiovasc Surg 132:918–924
15. Sekiya N, Matsumiya G, Miyagawa S, Saito A, Shimizu T, Okano T, Kawaguchi N, Matsuura N, Sawa Y (2009) Layered implantation of myoblast sheets attenuates adverse cardiac remodeling of the infracted heart. J Thorac Cardiovasc Sur 138:985–993
16. Gupta KB, Ratcliffe MB, Fallert MA, Edmunds LH Jr, Bogen DK (1994) Changes in passive mechanical stiffness of myocardial tissue with aneurysm formation. Circulation 89:2315–2326
17. Pfeffer MA, Braunwald E (1990) Ventricular remodeling after myocardial infarction. Experimental observations and clinical implications. Circulation 81:1161–1172
18. Mizuno T, Yau TM, Weisel RD, Kiani CG, Li RK (2005) Elastin stabilizes an infarct and preserves ventricular function. Circulation 112:81–88
19. Mizuno T, Mickle DA, Kiani CG, Li RK (2005) Overexpression of elastin fragments in infracted myocardium attenuates scar expansion and heart dysfunction. Am J Physiol Heart Circ Physiol 288:2819–2827
20. Keeley FW, Bellingham CM, Woodhouse KA (2002) Elastin as a self-organizing biomaterial: use of recombinantly expressed human elastin polypeptides as a model for investigations of structure and self-assembly of elastin. Philos Trans R Soc Lond B Biol Sci 357:185–189
21. Li DY, Brooke B, Davis EC, Mecham RP, Sorensen LK, Boak BB, Eichwald E, Keating MT (1998) Elastin is an essential determinant of arterial morphogenesis. Nature 393:276–280
22. Nakamura T, Lozano PR, Ikeda Y, Iwanaga Y, Hinek A, Minamisawa S, Cheng CF, Kobuke K, Dalton N, Takada Y, Tashiro K, Ross J Jr, Honjo T, Chien KR (2002) Fibulin-5/DANCE is essential for elastogenesis in vivo. Nature 415:171–175
23. Pereiral L, Lee SY, Gayraud B, Andrikopouls K, Shapiro SD, Bunton T, Biery NJ, Dietz HC, Sakai LY, Ramirez F (1999) Pathogenetic sequence for aneurysm revealed in mice underexpressing fibrillin-1. Proc Natl Acad Sci USA 96:3819–3823
24. Yanagisawa H, Davis EC, Starcher BC, Ouchi T, Yanagisawa M, Richardson JA, Olson EN (2002) Fibulin-5 is an elastin-binding protein essential for elastin fiber development in vivo. Nature 415:168–171
25. Kamoun A, Landeau JM, Godeau G, Wallach J, Duchesnay A, Pellat B, Hornebeck W (1995) Growth stimulation of human skin fibroblasts by elastin-derived peptides. Cell Adhes Commun 3:273–281
26. Wachi H, Seyama Y, Yamashita S, Suganami H, Uemura Y, Okamoto K, Yamada H, Tajima S (1995) Stimulation of cell proliferation and autoregulation of elastin expression by elastin peptide VPGVG in cultured chick vascular smooth muscle cells. FEBS Lett 368:215–219
27. Tajima S, Wachi H, Seyama Y (1996) Tropoelastin-derived degradation products down-regulate elastin expression in vascular smooth muscle cell in culture. Connect Tissue 28:231–235

28. Mecham RP, Hinek A, Entwistle R, Wrenn DS, Griffin GL, Senior RM (1989) Elastin binds to a multifunctional 67 kilodalton peripheral membrane protein. Biochemistry 28:3716–3722
29. Tyagi SC, Kumar SG, Alla SR, Reddy HK, Voelker DJ, Janicki JS (1996) Extracellular matrix regulation of metalloproteinase and antiproteinase in human heart fibroblast cells. J Cell Physiol 167:137–147
30. Brassart B, Fuchs P, Huet E, Alix AJ, Wallach J, Tamburro AM, Delacoux F, Haye B, Emonard H, Hornebeck W, Debelle L (2001) Conformational dependence of collagenase (matrix metalloproteinase-1) up-regulation by elastin peptides in cultured fibroblasts. J Biol Chem 276:5222–5227
31. Booms P, Ney A, Barthel F, Moroy G, Counsell D, Gille C, Guo G, Pregla R, Mundlos S, Alix AJ, Robinson PN (2006) A fibrillin-1-fragment containing the elastin-binding-protein GxxPG consensus sequence upregulates matrix metalloproteinase-1: biochemical and computational analysis. J Mol Cell Cardiol 40: 234–246
32. Lin X, Jo H, Ishii TM, Fujita M, Fu M, Tambara K, Yamamoto M, Tabata Y, Komeda M, Matsuoka S (2009) Controlled release of matrix metalloproteinase-1 plasmid DNA prevents left ventricular remodeling in chronic myocardial infarction of rats. Circulation 73:2315–2321
33. Matsumura S, Iwanaga S, Mochizuki S, Okamoto H, Ogawa S, Okada Y (2005) Targeted deletion or pharmacological inhibition of MMP-2 prevents cardiac rupture after myocardial infarction in mice. J Clin Invest 115:599–609
34. Noji Y, Shimizu M, Ino H, Higashikata T, Yamaguchi M, Nohara A, Horita T, Shimizu K, Ito Y, Matsuda T, Namura M, Mabuchi H (2004) Increased circulating matrix metalloproteinase-2 in patients with hypertrophic cardiomyopathy with systolic dysfunction. Circ J 68:355–360

Myoblast Sheet Can Prevent the Impairment of Cardiac Diastolic Function and Late Remodeling After Left Ventricular Restoration in Ischemic Cardiomyopathy

Shunsuke Saito,[1] Shigeru Miyagawa,[1] Taichi Sakaguchi,[1] Yukiko Imanishi,[1] Hiroko Iseoka,[1] Hiroyuki Nishi,[1] Yasushi Yoshikawa,[1] Satsuki Fukushima,[1] Atsuhiro Saito,[1] Tatsuya Shimizu,[2] Teruo Okano,[2] and Yoshiki Sawa[1,3]

Background. Impairment of diastolic function and late remodeling are concerns after left ventricular restoration (LVR) for ischemic cardiomyopathy. This study aims to evaluate the effects of combined surgery of myoblast sheets (MS) implantation and LVR.

Methods. Rat myocardial infarction model was established 2 weeks after left anterior descending artery ligation. They were divided into three groups: sham operation (n=15; group sham), LVR by plicating the infracted area (n=15; group LVR), and MS implantation with LVR (n=15; group LVR+MS).

Results. Serial echocardiographic study revealed significant LV redilatation and decrease of ejection fraction 4 weeks after LVR in group LVR. MS implantation combined with LVR prevented those later deteriorations of LV function in group LVR+MS. Four weeks after the operation, a hemodynamic assessment using a pressure-volume loop showed significantly preserved diastolic function in group LVR+MS; end-diastolic pressure (LVR vs. LVR+MS: 9.0±6.6 mm Hg vs. 2.0±1.0 mm Hg, $P<0.05$), end-diastolic pressure-volume relationship (LVR vs. LVR+MS 42±23 vs. 13±6, $P<0.05$). Histological examination revealed cellular hypertrophy and LV fibrosis were significantly less and vascular density was significantly higher in group LVR+MS than in the other two groups. Reverse transcription polymerase chain reaction demonstrated significantly suppressed expression of transforming growth factor-beta, Smad2, and reversion-inducing cysteine-rich protein with Kazal motifs in group LVR+MS.

Conclusions. MS implantation decreased cardiac fibrosis by suppressing the profibrotic gene expression and attenuated the impairment of diastolic function and the late remodeling after LVR. It is suggesting that MS implantation may improve long-term outcome of LVR for ischemic heart disease.

Keywords: Ischemic cardiomyopathy, Left ventricular restoration, Regenerative therapy, Myoblast sheet, Diastolic function.

(*Transplantation* 2012;93: 1108–1115)

Ischemic heart disease is one of the leading causes of death and disability in most of the industrialized countries and recognized as a major public health issue. Progression to end-stage heart failure involves massive loss of cardiomyocyte, massive fibrosis, and progressive remodeling of the ventricles. Left ventricular (LV) volume reduction surgery or LV restoration (LVR) surgery has been introduced as a surgical treatment of patients with dilated LV and chronic heart failure (*1*, *2*), and has been shown to reduce the LV volume, increase the ejection fraction, and improve ventricular function (*3*, *4*).

The authors declare no funding or conflicts of interest.

[1] Department of Cardiovascular Surgery, Osaka University Graduate School of Medicine, Suita, Osaka, Japan.

[2] Institute of Advanced Biomedical Engineering and Science, Tokyo Women's Medical University, Tokyo, Japan.

[3] Address correspondence to: Yoshiki Sawa, M.D., Department of Cardiovascular Surgery, Osaka University Graduate School of Medicine (E1), 2-2 Yamada-Oka, Suita, Osaka 565-0871, Japan.

E-mail: sawa@surg1.med.osaka-u.ac.jp

S.S. participated in research design, the performance of the research, data analysis, and the writing of the manuscript; T.S. participated in research design and data analysis; S.M. participated in research design and data analysis, and the writing of the manuscript; Y.I. performed quantitative analysis of engrafted myoblasts survival; H.I. performed histological analysis of engrafted myoblasts survival; H.N. participated in the performance of the research; Y.Y. participated in the performance of the research; S.F. participated in the performance of the research; A.S. participated in research design and data analysis; T.S. contributed to the development of the temperature-responsive culture dish and cell sheet implantation technique; T.O. contributed to the development of the temperature-responsive culture dish and cell sheet implantation technique; and Y.S. participated in research design, data analysis, and the writing of the manuscript.

Received 28 June 2011. Revision requested 20 July 2011.

Accepted 10 February 2012.

ISSN: 0041-1337/12/9311-1108

DOI: 10.1097/TP.0b013e31824fd803

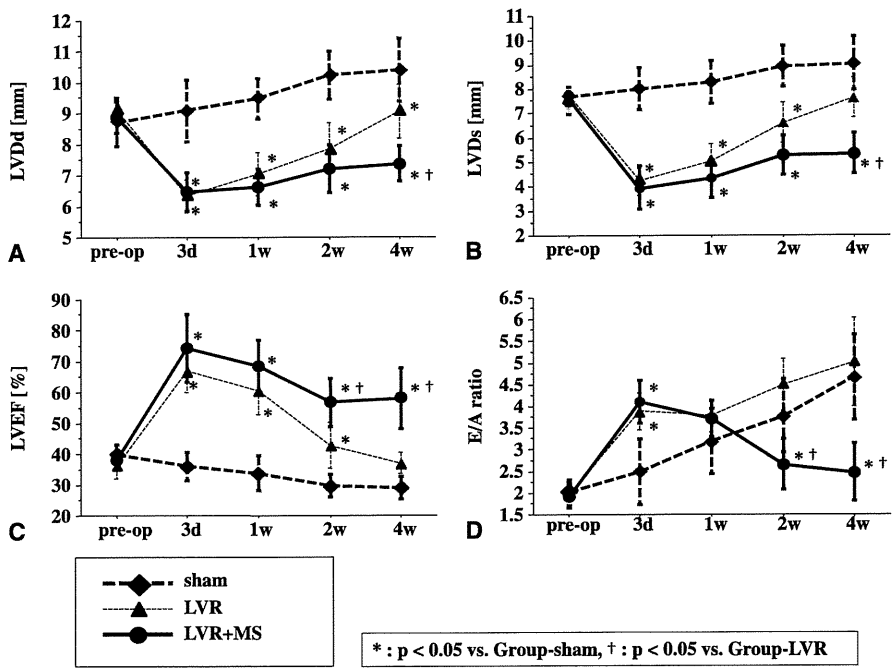

FIGURE 1. Serial echocardiographic study revealed significant decrease in left ventricular chamber size and significant increase in left ventricular ejection fraction by left ventricular restoration (LVR) in group LVR and in group LVR+ myoblast sheets (MS). However, gradual redilatation of left ventricular chamber and decrease of ejection fraction was observed in group LVR. Those later deteriorations were prevented in group LVR+MS, and the differences in chamber size and ejection fraction were significant between group LVR and group LVR+ MS 4 weeks after the operation. Changes in echocardiographic parameters before and after the operation. (A) Left ventricular dimension at end-diastole (LVDd), (B) left ventricular dimension at end-systole (LVDs), (C) Left ventricular ejection fraction (LVEF), (D) mitral valve E/A ratio. *P0.05 vs. group sham; †P0.05 vs. group LVR.

However, impairment of diastolic function and late remodeling are great concerns after LVR for ischemic cardiomyopathy (*5–7*), and the long-term effect of LVR is still controversial. Although LVR that is performed together with coronary artery bypass grafting (CABG) has been suggested to reduce the rate of hospitalization and improve ventricular function to a greater degree than CABG alone on the basis of a small, nonrandomized, case-control study (*8*), recently conducted multicenter, nonblinded, randomized trial (the Surgical Treatment for Ischemic Heart Failure [STICH] trial) have revealed that LVR does not improve the symptoms, exercise tolerance, rate of death, or hospitalization in patients with ischemic heart disease and severe LV dysfunction compared with CABG alone (*5*).

On the other hand, cell transplantation into impaired myocardium, also known as cellular cardiomyoplasty, has been investigated (*9*, *10*). Recently, we have developed a new cell delivery method by the means of cell sheet, in which autologous skeletal myoblasts were transplanted in sheet form, and reported that this method was effective especially in the attenuation of LV dilatation and the improvement of LV diastolic function (*11–14*). On the basis of these findings, we hypothesized that skeletal myoblast sheet (MS) implantation may attenuate the disadvantageous effects and enhance the advantageous effects of LVR. Using a rat model of chronic myocardial infarction model, we investigated whether MS implantation combined with LVR can attenuate the redilatation and diastolic dysfunction of LV after LVR.

RESULTS

Changes in Cardiac Function by LVR and LVR Combined With MS

Two weeks after left anterior descending coronary artery (LAD) ligation, severe dilatation of the LV chamber and severe asynergy of the anterior wall were observed in all the rats. By excluding the large akinetic or dyskinetic area of the LV anterior wall, LV dimension at end-diastole (LVDd) and end-systole (LVDs) significantly decreased and left ventricular ejection fraction (LVEF) significantly increased in group LVR and in group LVR+MS 3 days after treatment (Fig. 1). However, gradual LV redilatation and decrease of LVEF were observed in group LVR. MS implantation combined with LVR attenuated those later deteriorations of LV function significantly in group LVR+MS (Fig. 1). Mitral valve *E/A* ratio showed significant restrictive pattern after LVR. In group LVR, the restrictive pattern progressed even further with time. However, addition of the MS implantation attenuated the progression of the restrictive pattern (Fig. 1).

Hemodynamic Improvement by LVR Combined With MS

Table 1 shows the results of the hemodynamic study by cardiac catheterization 4 weeks after the second operation. The basic hemodynamic indices revealed that LV end-diastolic pressure (EDP) and the time constant of isovolumic relaxation (τ) were significantly lower in group LVR+MS than in group LVR or group sham. Load-independent parameters measured by pressure-volume loop analysis revealed that end-systolic pressure (ESP) volume relationship was significantly higher in group LVR+MS than in the other two groups. EDP volume relationship (EDPVR) was significantly lower in group LVR+MS than in the other two groups.

Histological Impact of the MS on the Failing Heart

Figure 2 shows the typical cross section of the whole hearts 4 weeks after the operation from each group. Severe dilatation of the LV chamber and thinning of the LV wall were observed in group sham (Fig. 2A). In group LVR, although infracted area was excluded and smaller than that in group sham, LV chamber was markedly dilated (Fig. 2B). Also severe dilatation of the right ventricular chamber was observed. In group LVR+MS, the size of the LV chamber and the thickness of the LV wall were well preserved compared

TABLE 1. Hemodynamic indices 4 weeks after the operation

Group	Sham	LVR	LVR+MS
Basic hemodynamic indices			
HR (bpm)	219 ± 37	206 ± 20	231 ± 32
ESP (mm Hg)	60.9 ± 7.7	63.0 ± 13.9	73.0 ± 11.3[a]
EDP (mm Hg)	5.1 ± 2.2	9.0 ± 6.6	2.0 ± 1.0[a,b]
τ (msec)	21.3 ± 2.4	19.8 ± 2.2	14.4 ± 1.2[a,b]
Load independent parameters analyzed by pressure-volume loop			
ESPVR (mm Hg/ml)	1896 ± 906	1364 ± 661	4722 ± 2416[a,b]
EDPVR (/ml)	50 ± 36	42 ± 23	13 ± 6[a,b]
PRSW (mm Hg)	37.1 ± 24.3	33.0 ± 24.2	45.2 ± 32.7

[a] $P < 0.05$ vs. group sham.
[b] $P < 0.05$ vs. Group-LVR.
HR, heart rate; ESP, end-systolic pressure; EDP, end-diastolic pressure; τ, time constant of isovolumic relaxation; ESPVR, end-systolic pressure-volume relationship; EDPVR, end-diastolic pressure-volume relationship; PRSW, preload-recruitable stroke work.

with the other groups (Fig. 2C). The LV wall thickness was significantly larger in group LVR+MS than in the other two groups (vs. group sham and group LVR, $P<0.05$) (Fig. 3A). The degree of cardiac fibrosis was significantly smaller in group LVR+MS than in the other two groups (vs. group sham and group LVR, $P<0.05$) (Figs. 3B and 4A–C). Myocyte size was also significantly smaller in group LVR+MS than in the other two groups (vs. group sham and group LVR, $P<0.05$) (Figs. 3C and 4D–F). Vascular density of the LV lateral wall, the area where MS were applied in group LVR+MS, was significantly higher in group LVR+MS than in the other two groups (vs. group sham and group LVR, $P<0.05$) (Figs. 3D and 4G–I).

Suppression of Probrotic Agent Gene Expression by MS

Reverse transcription polymerase chain reaction analysis 4 weeks after the second operation revealed significantly suppressed expression of the profibrotic gene transforming growth factor-beta (TGF-β), Smad2, and reversion-inducing cysteine-rich protein with Kazal motifs (RECK) in group LVR+MS than in the other two groups (vs. group sham and group LVR, $P<0.05$) (Fig. 5A–C).

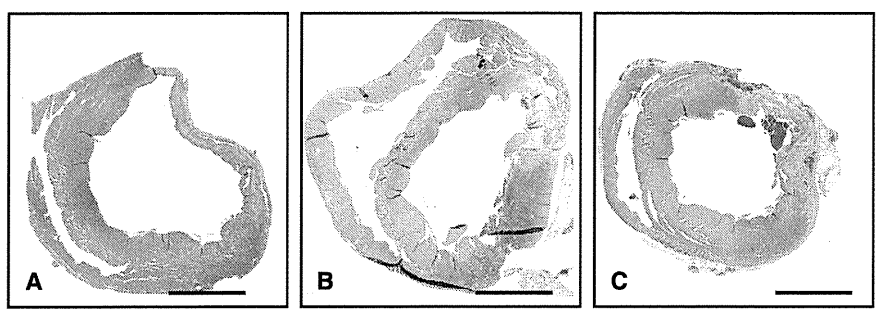

FIGURE 2. Cross section of the whole hearts 4 weeks after the operation from each group (hematoxylin-eosin staining). (A) group sham, (B) group LVR, (C) group LVR + MS.

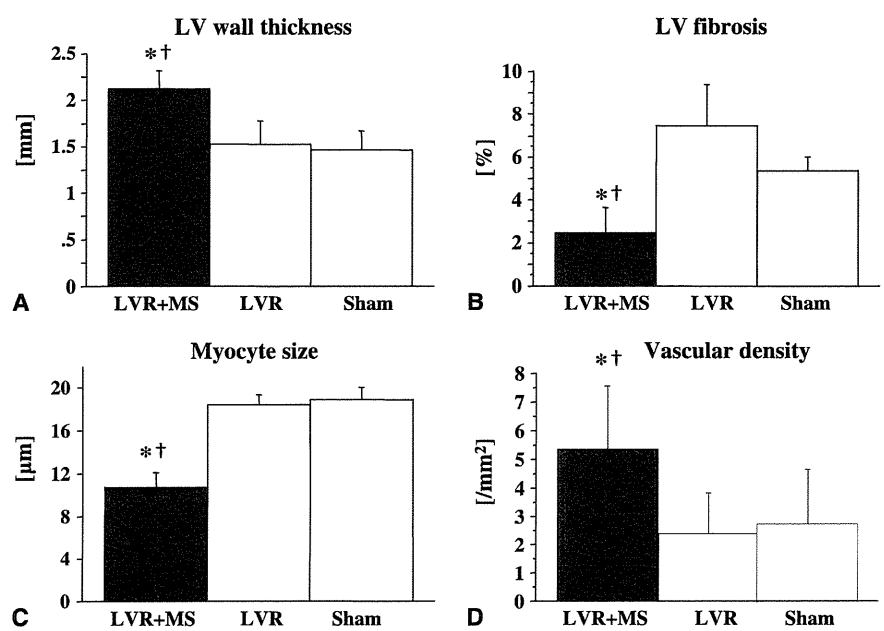

FIGURE 3. The left ventricular (LV) wall thickness was significantly larger in group left ventricular restoration (LVR)+myoblast sheets (MS) than in the other two groups 4 weeks after the operation (A). The degree of cardiac fibrosis (B) and myocyte size (C) were also significantly smaller in group LVR+MS than in the other two groups. The vascular density in the LV lateral wall, where MS were applied in group LVR+MS, were significantly higher in group LVR+MS than in the other two groups (D).

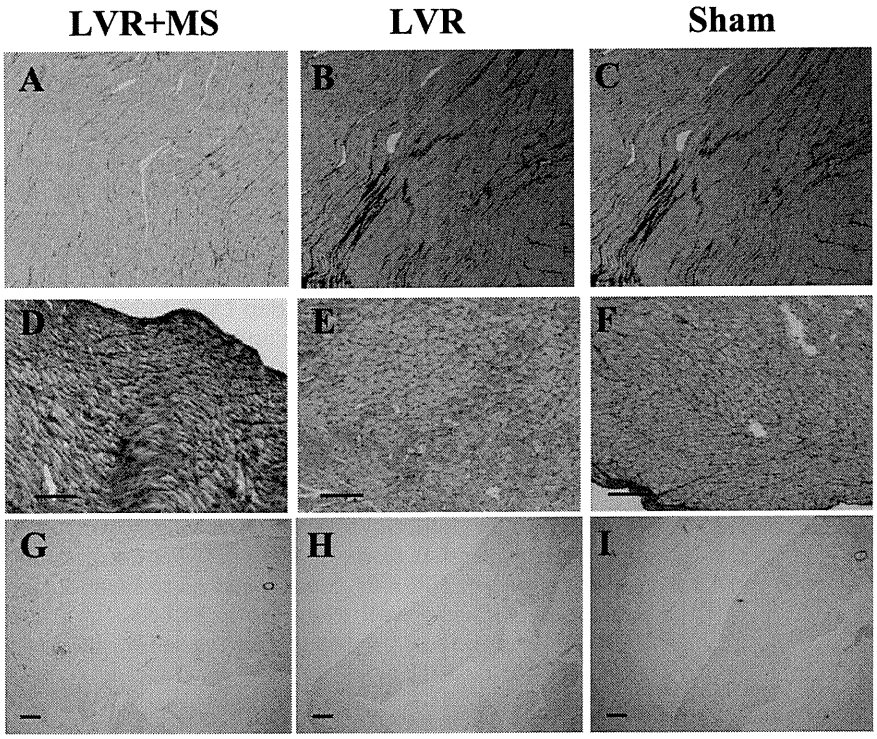

FIGURE 4. Picrosirius-red staining of myocardium from noninfarcted regions (A, B, C) and periodic acid-Schiff-stained myocardium from noninfarcted regions (D, E, F, bar=200 μm). Picrosirius-red staining of myocardium from noninfarcted regions. Sections of myocardium stained with antibody to von Willebrand factor (G, H, I, bar=300 μm).

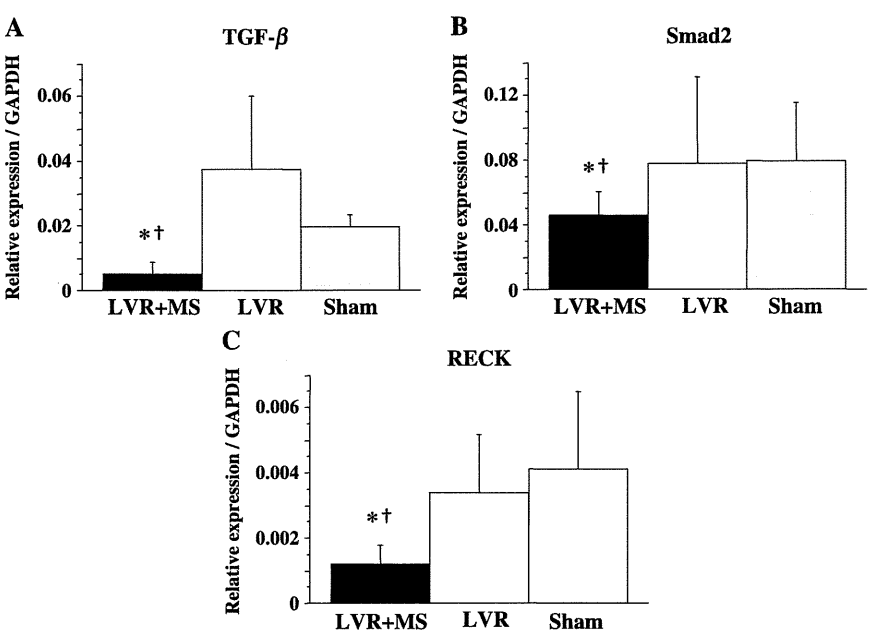

FIGURE 5. Reverse transcription polymerase chain reaction (RT-PCR) analysis 4 weeks after the second operation revealed significantly suppressed expression of the profibrotic gene transforming growth factor-beta (TGF-β) (A), Smad2 (B), and RECK (C) in group left ventricular restoration (LVR)+myoblast sheets (MS) than in the other two groups.

Engrafted Cell Survival

To evaluate the survival of engrafted cell on the recipient LV, MS made from male rats were implanted on the female LV, and surviving cell numbers were examined by detecting the Y chromosome-specific and gender consensus genes. To confirm the accuracy of the measurements, MS made from known numbers of male myoblasts were implanted on the LV wall of a female rat ex vivo, and a standard curve was prepared to determine the ratio of male cells to female cells and the relationship to the number of male cells. The correlation coefficient for the standard curve was 0.9716, indicating a significant correlation. The number of surviving engrafted cells was calculated using this standard curve (*15*). The number of cells detected on the day of implantation was approximately 64% of the engrafted cells (five layers of MS, with 3.0×10^6 myoblasts in each sheet). Surviving cells decreased to 69% of those in day 0. Although the number continued to decrease with time, 13% of those cells were still surviving on the LV wall 4 weeks after MS implantation (Fig. 6A).

Immunostaining of the green fluorescent protein (GFP) revealed that myoblasts sheets made from GFP transgenic rats